Effect of Concentration on Reaction Kinetics in Polymer Solutions

Ben O'Shaughnessy

Department of Chemical Engineering, Materials Science and Mining Engineering, Columbia University, New York, New York 10027

Received June 30, 1993; Revised Manuscript Received March 1, 1994[⊕]

ABSTRACT: We present a theory of irreversible interpolymeric reaction rates k as a function of polymer concentration ϕ in polymer solutions ranging from dilute through to the melt. At high dilution, kinetics obey mean-field (MF) theory such that k scales as the equilibrium reactive group contact probability. k thus grows with increasing concentration, since the contact probability is enhanced due to screening of excluded volume repulsions: $k \sim \phi^{3g/4}$ where g is the monomer contact exponent. At large concentrations kinetics are radically different: $k \approx R^3/\tau$ then follows a "diffusion-controlled" (DC) law and decreases with increasing ϕ since both coil size R and relaxation rate $1/\tau$ are diminished. This leads to $k \sim \phi^{-5/8}$ (unentangled solutions) or $k \sim \phi^{-(5/8+\gamma)}$ (entangled solutions) where γ is the entanglement exponent. The transition from MF to DC kinetics happens because the total reaction probability P during one coil–coil collision is always an increasing function of ϕ. k is peaked at the transition concentration ϕ^{**}, where P reaches unity for the first time. In agreement with experiment, ϕ^{**} is distinct from the overlap threshold.

I. Introduction

The aim of this paper is the development of a basic theory describing the influence of polymer concentration on interpolymeric reaction kinetics (see Figure 1). Perhaps the most significant application is linear free radical polymerization[1-7] in which termination through "chain coupling" consists of irreversible intermolecular reaction between polymers bearing highly reactive radical ends in an environment which is initially dilute in terminated (dead) polymer chains. As polymerization proceeds, the dead polymer concentration grows, passing into the semidilute regime and ultimately into the melt. Clearly, one needs the dependence of reaction rate constants on *chain length* and *polymer concentration* in order to understand these and other[1] polymerization processes. Beyond polymerization, the form of interpolymeric rate constants has been measured by conventional chemical techniques[14] and in numerous studies employing photophysical methods[8-13] as a probe of fundamental polymer behavior, and is crucial to the dynamics of "reacting" systems such as surfactant solutions in which molecules aggregate into long flexible chains[15,16] ("wormlike micelles").

Movitated thus, we will analyze the following problem. We consider a solution of polymers in good solvent, each chain of N units, at concentration c (chain units per unit volume) or equivalently polymer volume fraction $\phi \approx ch^3$ where h is the size of one chain unit. A small fraction of these chains are "live", bearing one reactive group (see Figure 1), and can react irreversibly with one another. The emphasis here is on highly reactive groups (small activation energies), but our results cross over smoothly to the weakly reactive case. We assume the number density of live chains, n, decreases in time according to second order reaction kinetics

$$\dot{n} = -kn^2 \tag{1}$$

where k is the reaction rate constant. The main objective of this study is to establish the dependence on N and ϕ, $k(N,\phi)$.

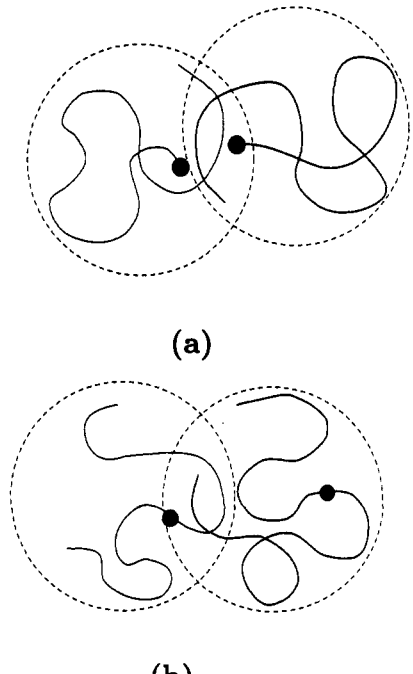

Figure 1. If center-of-gravity diffusion brings two live coils together as depicted, reaction may occur during the period (of order τ, the longest coil relaxation time) for which the coils remain interpenetrated. The reaction probability during a single such encounter depends on whether the number of collisions, $\mathcal{N}^{coll}$, between the reactive groups during τ (see eqs 6, 7, and 9) is an increasing or a decreasing function of chain length; these two possibilities lead respectively to DC and MF kinetics. The cases of end groups and internal groups are shown in (a) and (b) respectively. Since internal groups suffer the stronger excluded volume repulsions (the exponent g is larger), reaction rates are characterized by different exponents (compare eqs 42 and 43).

The two extremes of concentration are melts, $\phi = 1$, and dilutes solutions, $\phi < \phi^*$, where $\phi^* \approx N^{-4/5}$ is the chain overlap threshold defining the onset of the semidilute regime.[17,18] A coherent theoretical picture has been developed for reaction kinetics in these two cases,[19-22] described in detail in ref 22. Our objective here is the range of concentrations between these two limits, and we will borrow many concepts from the dilute and melt cases. According to theory, the essential difference between these

[⊕] Abstract published in *Advance ACS Abstracts*, May 15, 1994.

0024-9297/94/2227-3875$04.50/0

two extremes is that reactions are "strong" in melts and "weak" in dilute solutions. In melts, kinetics are intrinsically "diffusion-controlled" (DC) in that, for large enough N, two live polymers will almost certainly react with one another should center of gravity diffusion overlap their respective coil volumes (see Figure 1). That is, reaction occurs if the functional groups diffuse to within a distance R of one another, where R is the rms polymer coil size. This leads to[19,20,22] $k \approx R^3/\tau$ where τ is the longest polymer relaxation time; only the large polymer scales feature in k (all chemical and physical details of the reactive groups disappear). In fact, rewriting this as $k \approx DR$ ($D \approx R^2/\tau$ being the polymer center of gravity diffusion coefficient), one recognizes this[23] as the diffusion-controlled Smoluchowski result[24] for small molecules with the "capture radius" (i.e., the reaction range) replaced by the coil size R.

A coil–coil collision in dilute solution (good solvents) is by contrast unlikely to result in reaction, for large N. This is true even if the functional groups are themselves highly reactive and results from two important effects absent in melts. First, the collision time, essentially the coil relaxation time τ, is reduced by hydrodynamical interactions; there is less time to react. Second, during this period the number of collisions between the reactive groups is significantly reduced by *excluded volume repulsions*; while the two coils can interpenetrate significantly,[17,25] it is well-known that the equilibrium contact probability between two chain units, one belonging to each polymer, is diminished:

$$P_{eq}^{cont} \approx \frac{h^3}{V}\left(\frac{h}{R}\right)^g \qquad (2)$$

where V is the volume of the reaction vessel. This is the "correlation hole" effect,[17,25,26] and the reduction factor relative to melts, $(h/R)^g$, is governed by des Cloizeaux's "correlation hole" exponent g. It happens that the total reaction probability during one collision between a pair of live coils is rendered very small by these reductions in τ and P_{eq}^{cont}. This means that pair correlation functions between the reactive units of different chains are little disturbed from their equilibrium forms. Hence reaction rates are proportional to the *equilibrium* contact probability P_{eq}^{cont}; in other words mean-field (MF) theory is applicable since reaction-induced correlations turn out to be unimportant. One may view MF kinetics as a generalization of the "law of mass action" (LMA) under which reaction rates for small molecules are proportional to equilibrium contact probabilities. In previous works we have equivalently used the labels LMA (e.g., refs 27 and 28) and MF (ref 22) to denote this type of reaction kinetics. We shall adhere to the term MF in the present study.

As will be shown, an important distinguishing feature of MF kinetics is that while k scales[22,28] with a universal power of molecular weight, its prefactor involves the physical and chemical details of the functional groups. In our model these are the *local* reaction rate Q, measured in s^{-1} (i.e., the reaction rate given that the functional groups overlap one another) and the size of the groups h. We can think of kinetics as being "reaction-controlled" rather than "diffusion-controlled". Notice that the exponent g plays an important role when MF kinetics apply. It is through g that the dependence on reactive group location arises (see Figure 1): when both functional groups are at chain ends[29,30] $g \approx 0.27$; for one end and one internal group $g \approx 0.43$; for both internal $g \approx 0.80$.

In summary, kinetics in melts are intrinsically DC, in dilute solutions intrinsically MF where "intrinsically" here translates into "large N". Just how large N must be depends on the magnitude of Q. For example, melts of moderately long chains exhibit MF kinetics for small Q (substantial activation barrier). However, at sufficiently large N this behavior inevitably *crosses over* from MF to DC. The smaller Q, the larger the crossover molecular weight. (For sufficiently tiny Q this cross-over becomes unphysically large and MF kinetics will then always prevail.) We will examine this transition in section IV.

Let us consider what is known experimentally about k as concentration increases from dilute solution toward the melt. Free-radical polymerization measurements (which involve "large-Q" reactions) such as those of North and Reed[31] suggest that initially k exhibits an increase. Recently, Kent et al.[32] have argued that this derives from the reduced interpolymeric repulsion and increased coil–coil overlap time which accompany increased concentration,[17,33] serving to enhance reaction probability when two coils collide and thereby increase k. Meanwhile, the general picture[1] from free-radical polymerizations at higher concentrations is that k drops dramatically, ultimately leading to the celebrated gel or Trommsdorff effect[1,34] when termination rates are so reduced due to increased viscosity that chain growth autoaccelerates into an entangled melt.

Photophysical measurements[11] provide more unambiguous information. Gebert and Torkelson[35] have found that phosphorescence quenching (large Q) rates in end-labeled polymer solutions at large concentrations decrease with increasing ϕ. Similar observations were made by Mita et al.[10,11] who reported a rather novel behavior. In good solvents, after an initial increase as ϕ increased into the semidilute regime, k was observed to *peak* at a certain value of ϕ and then decay monotonically for greater values (see Figure 2a). For the longest chains the peak did not appear to coincide with ϕ^*.

The rest of this paper aims to explain this type of experimental behavior. We will find that the peak in k is due to a transition, caused by increasing concentration, from MF to DC kinetics.[36] At low concentrations the dilute MF kinetics are obeyed. Therefore the determinant of reaction rate is the contact probability P_{eq}^{cont}. But with increasing ϕ excluded volume repulsions are increasingly *screened out*,[17] causing P_{eq}^{cont} and thus k to increase. On the other hand, at high concentrations kinetics are of DC type. Hence $k \approx R^3/\tau$ *decreases* with increasing ϕ since the coil size diminishes (excluded volume swelling being screened out) as does the relaxation rate. It follows that k is peaked somewhere between these dilute-like and melt-like regimes.

Why does this $MF \rightarrow DC$ transition occur? Because the increase in P_{eq}^{cont} at low concentrations has a second effect: it increases the total reaction probability during each coil–coil encounter. Eventually, this reaches unity; then live coils react whenever they meet, i.e., one has DC kinetics. The concentration at which the total reaction probability equals unity is the location of the peak.

In section II a general expression for k will be derived which involves[20] the group–group "return probability" $S(t)$, namely, the probability that the reactive groups belonging to two interpenetrating live coils are in contact at time t given initial contact. Section III establishes the general form of $S(t)$ which is used in section IV to derive k for the two extreme regimes of melts and dilute solutions. In the following two sections the dependence of k on concentration is studied, beginning with polymers short enough to

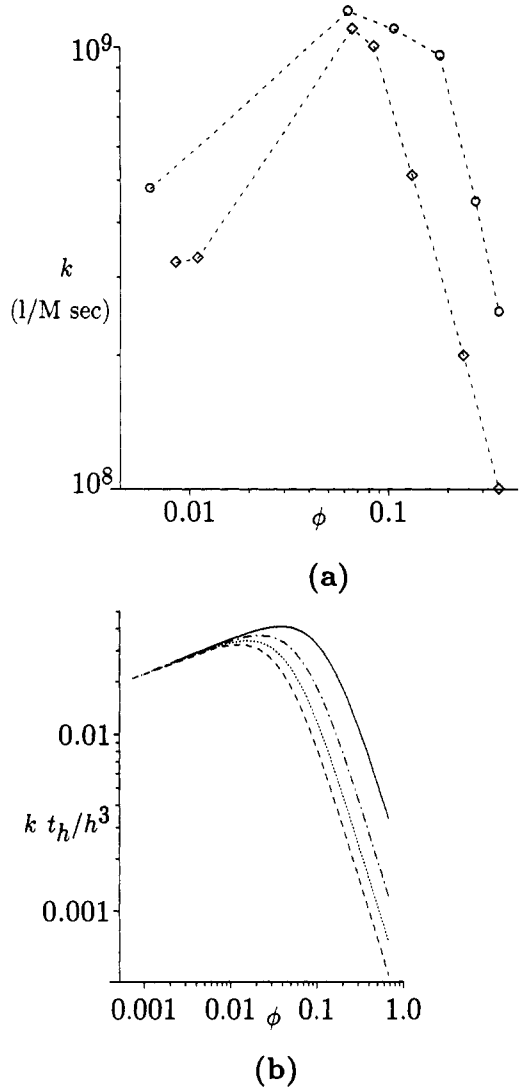

Figure 2. Logarithmic plots of k versus ϕ for reactive groups at chain ends. (a) Experimental phosphorescence quenching rates taken from ref 10 for polystyrene, end-capped with benzil and anthryl groups, in benzene solvent at 30 °C. ○: reacting chains of 800 and 640 units, inert background chains 1000 units. ◇: background 3800 units, reacting chains 3900 and 2900 units (four smallest ϕ values) and 3300 and 1200 units (three largest ϕ values). Estimated values of ϕ^* are 0.006 (○) and 0.002 (◇). All ϕ values are calculated using the estimate h = 5.5 Å from ref 50. (b) Theoretical dimensionless rate constant kt_h/h^3, against ϕ values ranging from ϕ^* into the semi-dilute regime, for four "weak" systems (eqs 37 and 42). Dimensionless group reactivity $\tilde{Q}t_h$ = 0.1, N = 4000 (solid line), N = 8000 (dash–dotted line), N = 12 000 (dotted line) and N = 16 000 (dashed line). Entanglement parameters are N_e = 200 and γ = 1. The MF to DC transition occurs at $\phi^{**}_{ent} \approx$ 0.07, 0.04, 0.03, 0.02 for the four N values respectively.

be unentangled in section V. Entanglement effects are dealt with in section VI in the framework of the reptation model. In section VII we classify a given reacting polymer system as either "weak" or "strong" depending on whether entanglements onset before or after the MF → DC transition; our experimental predictions are somewhat different for these two classes of system. In section VIII we conclude by discussing our results and comparing them with experimental measurements.

II. General Expression for Rate Constant k

Writing $n(t) \equiv M(t)/V$ where $M(t)$ is the number of unreacted live chains in the reaction vessel after time t, we have $\dot{M} \approx -\dot{\Gamma}_t M^2$ where Γ_t is the fraction of live pairs which have reacted by the time t, $\Gamma_t \equiv 1 - \int d^3r\, P_t(r)$, and $P_t(r)$ is the probability at time t that a given pair of live chains have not yet reacted and that their functional groups are separated by r. Equation 1 then implies $k = V\dot{\Gamma}_t$.

We have chosen our chain unit size, h, to match the reaction range of the active groups. Thus one unit of each live chain is reactive, and irreversible reaction occurs with probability Q per unit time should the reactive units of two chains overlap ($r < h$). This leads to the following self-consistent expression for the pair distribution function:

$$P_t(r) \approx P_{eq}(r) - Q\int_0^t dt' \int_{|r'|<h} d^3r'\, G(r,r',t-t')\, P_t(r') \quad (3)$$

where $P_{eq}(r)$ is the initial equilibrium distribution and $G(r,r',t-t')$ the usual Green's function for nonreactive polymers, that is the normalized conditional probability density of separation r at t, given that the separation at t' was r'. This is essentially the Wilemski and Fixman reaction model which has been used in many theoretical studies,[20,37-39,40] and the derivation of eq 3 is thoroughly discussed by de Gennes in ref 20. It states that the number of unreacted polymer pairs whose reactive groups are separated by r, namely, $P_t(r)$, equals the number there would have been had there been no reactions ($P_{eq}(r)$) minus the number of pairs which have reacted since t = 0. This latter quantity is expressed self-consistently as a sum over all possible reaction times t' and group separations r' at the time of reaction.

Equation 3 is not exact; implicitly, it involves the self-consistent "closure approximation" of Wilemski and Fixman. In fact the coordinate r does not decouple from all other polymer chain degrees of freedon and the approximation amounts to assuming equilibrium configurations for chains with overlapping functional groups.[40] However, there is very strong evidence that the resulting errors are small and that eq 3 leads to the correct dependencies of k on molecular weight. Doi has used the above scheme to calculate both cyclization rates[38] and intermolecular reaction rates[19] assuming Rouse dynamics (describing polymers in unentangled melts). "First principles" renormalization group (RG) treatments of the same two problems,[22,27,41] in which these approximations are not used, lead to the identical molecular weight exponents α, k = constant·$N^{-\alpha}$. The only differences arise in the constant prefactor. The results obtained by de Gennes, using the same self-consistent framework, for the short-time kinetics of reacting Rouse chains are similarly supported by RG analyses[42] which give the same powers of time t, but slightly different prefactors. We will present further evidence in section IV, where eq 3 will be employed to calculate k for dilute solutions. The expressions obtained are once again in agreement with those of ref 22 based on RG methods. The RG analyses show that the success of this approximation scheme lies in the fact that a reaction sink is a weak perturbation, in the sense that it does not modify static and dynamic exponents.

Solving eq 3 for the normalization of $P_t(r)$, namely Γ_t, and using $k = V\dot{\Gamma}_t$ one obtains the following result for the long time rate constant (see Appendix A):

$$k = \frac{QVP_{eq}^{cont}}{1 + Q\int_0^\infty dt\, S(t)} \quad (4)$$

in which the crucial quantity is the time integral of the return probability $S(t)$ in the absence of reactions, defined as

$$S(t) \equiv \int_{|r|<h} d^3r\, G(r,0,t) \quad (5)$$

In melts ($P_{eq}^{cont} \to h^3/V$) and for $Q \to \infty$, eq 4 matches the expression obtained by de Gennes.[20] The power of this result is that it relates the nonequilibrium property k to static and dynamic properties of the *equilibrium* state, namely, P_{eq}^{cont} and $S(t)$. For the remainder of this paper we will use eq 4 to deduce k for different regimes of concentration and chain length. Now the static equilibrium property P_{eq}^{cont} is well-known,[17,25] and the appropriate forms will be presented for each concentration regime as we need them. Therefore, our first task is to derive the return probability $S(t)$ in these different regimes. In melts, where reactive groups belonging to different chains are statistically independent of one another due to screening[17] effects, $S(t)$ was calculated by de Gennes.[20] Its general form, including situations where interpolymic correlations exist, has not to our knowledge been previously derived. This will be done in section III.

Let us first develop a few simplified arguments which help to clarify the meaning of the general result for k in eq 4. Now the time integral of the return probability is proportional to the total number of collisions between a pair of "reactive" monomers which are initially in contact, but with their reactivity switched off. The two "reactive" monomers belong to two different polymers. Thus

$$\int_0^\infty S(t)\, \mathrm{d}(t/t_h) \approx B + \mathcal{N}^{\mathrm{coll}}, \qquad \mathcal{N}^{\mathrm{coll}} \approx \frac{\tau}{t_h} P_{eq}^{cont} \frac{V}{R^3} \quad (6)$$

where $\mathcal{N}^{\mathrm{coll}}$ is the mean number of collisions (each lasting t_h, the monomer relaxation time) between the "reactive" monomers of two chains when they encounter one another through center of gravity diffusion (Figure 1). $\mathcal{N}^{\mathrm{coll}}$ is defined to be an average over all initial overlapping equilibrium configurations, while $S(t)$ refers to a very specific initial situation in which the groups are in contact. Thus one picks up roughly one extra collision; this is the constant B, of order unity. We have estimated $\mathcal{N}^{\mathrm{coll}}$ as the number of time steps during one interpolymeric collision, namely, τ/t_h, multiplied by the fraction of these collisions for which the reactive groups are in contact. This fraction equals the conditional contact probability given coil overlap, i.e., P_{eq}^{cont} divided by the coil overlap probability R^3/V.

Equation (6) will be verified later. It leads to

$$k = \frac{\tilde{Q} V P_{eq}^{cont}}{1 + \tilde{Q} t_h \mathcal{N}^{\mathrm{coll}}}, \qquad \tilde{Q} \equiv \frac{Q}{1 + BQt_h} \quad (7)$$

in which $\tilde{Q} t_h \mathcal{N}^{\mathrm{coll}}$ is a measure of the total *reaction probability* P during a single coil–coil collision. That is, $P \approx \tilde{Q} t_h \mathcal{N}^{\mathrm{coll}}$ when $\tilde{Q} t_h \mathcal{N}^{\mathrm{coll}} \ll 1$, and $P \approx 1$ when $\tilde{Q} t_h \mathcal{N}^{\mathrm{coll}} \gg 1$. The meaning of the effective local reactivity $\tilde{Q}$ will be discussed shortly. Using our estimate for the number of collisions, one has

$$\frac{1}{k} = \frac{1}{k^{\mathrm{MF}}} + \frac{1}{k^{\mathrm{DC}}}$$

$$k^{\mathrm{MF}} \equiv \tilde{Q} V P_{eq}^{cont}, \qquad k^{\mathrm{DC}} \equiv R^3/\tau \quad (8)$$

This has a very familiar structure, describing kinetics in which the slowest of the MF and DC processes dominates k. Whether MF or DC kinetics pertain depends on the total reaction probability when two coils collide, in turn governed by the number of collisions $\mathcal{N}^{\mathrm{coll}}$. This is very clear from eq 7. If this probability is very small, $\tilde{Q} t_h \mathcal{N}^{\mathrm{coll}} \ll 1$, one obtains $k = k^{\mathrm{MF}}$; equilibrium is only very weakly perturbed by the reactions and the MF law follows. But if $\tilde{Q} t_h \mathcal{N}^{\mathrm{coll}} \gg 1$, then $k = k^{\mathrm{DC}}$ follows; reaction is then ensured if ever two live coils collide and equilibrium is strongly disturbed. Note that the MF law involves not Q but $\tilde{Q}$, which can never exceed t_h^{-1}. This is sensible, reflecting the fact that reactions cannot proceed more rapidly than the diffusion rate t_h^{-1} itself.

Reaction kinetics differ from one regime to another because the number of collisions $\mathcal{N}^{\mathrm{coll}}$ either becomes very large or very small for very long chains. It turns out that the $N \gg 1$ behavior is governed by a characteristic exponent as follows. Using the expression for the contact probability eq 2, and noting the definition[17] of the dynamical exponent z, $\tau/t_h = (R/h)^z$, one has

$$\mathcal{N}^{\mathrm{coll}} \approx (\tau/t_h)^{1-\theta} \quad (9)$$

where the "reaction exponent" is defined as[42,43]

$$\theta = (3 + g)/z \quad (10)$$

For very large N, one has $\tau/t_h \gg 1$. Therefore reaction kinetics are always DC when $\theta < 1$ and always MF when $\theta > 1$. The class of the asymptotic reaction kinetics depends only on θ, no matter what the group reactivity Q may be.

Consider two examples, beginning with unentangled melts. Here the correlation hole is screened out ($g = 0$) and the dynamics are Rouse-like ($z = 4$), which means that $\theta < 1$. Hence k is *driven* to DC form[22] for long chains. Dilute solutions with good solvent exhibit the "opposite" MF kinetics because[17] g is nonzero and $z = 3$, whence $\theta > 1$. That is, no matter how strongly reactive the functional groups may be the DC limit is not realized.[28]

In the following section we will justify these simplified arguments by establishing the general form of $S(t)$. The exponent θ arises naturally.

III. Structure of Return Probability $S(t)$

This section is concerned with $S(t)$ for situations where interpolymeric correlations may be present. Generally, equilibrium correlations are governed by the exponent g which determines the behavior of the pair distribution function:[17]

$$P_{\mathrm{eq}}(r) \sim r^g \quad (11)$$

for small values of the separation r between the reactive chain units. Due to excluded volume repulsions, the probability density vanishes at the origin. Melts are a special case where correlations disappear, $g = 0$.

$S(t)$ is the probability that two chain units belonging to different polymers are in contact at time t, given they were initially in contact, in the *absence* of reactions. To determine its form we will invoke three principles, the first being detailed balance which dictates that

$$P_{\mathrm{eq}}(r')\, G(r,r',t) = P_{\mathrm{eq}}(r)\, G(r',r,t) \quad (12)$$

Second, we assert that $G(r,r',t)$ is approximately independent of r' for values of r' much less than the rms distance diffused by each chain unit after time t, namely, $x_t \approx h(t/t_h)^{1/z}$. This is simply the principle of finite memory: the initial condition r' will be forgotten after a time scale much greater than the diffusion time corresponding to r', i.e., when the width of G as a function of r greatly exceeds r', one may simply replace r' with zero. Then, specializing eq 12 to small values of r and r', we obtain

$$\frac{G(r,0,t)}{P_{eq}(r)} = \frac{G(r',0,t)}{P_{eq}(r')} \qquad (r,r' \ll x_t) \tag{13}$$

Since this must be true for all small values of r and r', we conclude that $G(r,0,t)/P_{eq}(r)$ is *independent* of r for $r \ll x_t$, i.e., the small r behavior of G must match that of $P_{eq}(r)$ displayed in eq 11. That is, $G(r,0,t) = r^g f(t)$ for some function $f(t)$. Finally, let us assume that the only scales in G are r and x_t. Then the dimensions of G force the following structure:

$$G(r,0,t) \approx \frac{1}{x_t^3}\left(\frac{r}{x_t}\right)^g \qquad (r \ll x_t) \tag{14}$$

This result is physically reasonable; $G(r,0,t)$ is essentially equal to the conditional equilibrium probability that the groups are separated by r, given that they lie within x_t of each other.[28] That is, the dynamics of the relative position of the reactive groups are ergodic in a region of volume x_t^3 only, so within that portion of r-space relative probabilities are *as in equilibrium*. Inserting the above form for G into the definition of $S(t)$, eq 5, one arrives at the following scaling form involving the reaction exponent of eq 10:

$$S(t) \sim t^{-\theta} \tag{15}$$

"Switching off" correlations, $g \to 0$, one recovers de Gennes' result of ref 20. This general relation will enable us to calculate the rate constant through eq 4 which involves the time integral of $S(t)$.

Before specializing to different regimes of polymer concentrations, each involving different values of θ, we can make a general statement about the long-time behavior of $S(t)$. On time scales much greater than the longest polymer relaxation time Fickian center of gravity diffusion takes over, $z = 2$. Correspondingly, on scales much greater than the coil size all interpolymeric correlations are lost ($P_{eq}(r) \to 1/V$ independent of r), i.e., $g = 0$. Thus[20]

$$S(t) \sim t^{-3/2} \qquad (t \gg \tau) \tag{16}$$

For these large scales the return probability scales as the inverse volume explored, $1/x_t^3$, where $x_t \sim t^{1/2}$. The strong decay guarantees the existence of the time integral and thus of k according to eq 4.

IV. The Extremes: Melts and Dilute Solutions

The arguments of section II suggest that in order to obtain k our main task is to determine how many times two reactive groups will collide when their host coils collide. This is $\mathcal{N}^{coll}$ of eq 9, itself determined by the "reaction exponent" θ of eq 10. The result of eq 7 then gives k.

Let us begin by confirming that these arguments are correct for melts and dilute solutions, starting from the scaling form derived in the previous section for the return probability, eq 15, which involves θ. Generally, even for a given concentration regime, θ has different values at short and long times. Noting from the definition of eq 5 that the short time divergence of $S(t)$ is cut off at t_h, i.e., the return probability equals unity for shorter times, and demanding continuity in $S(t)$, eqs 15 and 16 lead immediately to the following form:

$$S(t) \approx \begin{cases} 1, & t < t_h \\ (t/t_h)^{-\theta}, & t_h < t < \tau \\ (\tau/t_h)^{-\theta}(t/\tau)^{-3/2}, & t > \tau \end{cases} \tag{17}$$

where θ above denotes the exponent relevant to short times $t_h < t < \tau$. Integrating $S(t)$, one recovers the results of eqs 6 and 9, where the constant B is identified as the contribution from times $t \lesssim t_h$. This verifies the expression for k presented in eq 7.

A. Melts ($\theta < 1$). Consider first melts of chains shorter than the entanglement[17,18,44] threshold N_e^{melts}, where dynamics are of Rouse type, $\tau \approx t_h N^2$ or $z = 4$, and statics are ideal, $R \approx hN^{1/2}$ and $g = 0$. This implies $\theta = 3/4$, and from eq 9 one therefore has

$$\mathcal{N}^{coll} \approx (\tau/t_h)^{1/4} \approx N^{1/2} \qquad \text{(unentangled)} \tag{18}$$

In unentangled melts, a reactive pair will collide a very large number of times if their host coils should happen to collide. For a given local reactivity Q, provided chains are much longer than a certain length N_{un}^*, reaction is then guaranteed. This length is obtained by equating the total reaction probability to unity, $\tilde{Q}t_h\mathcal{N}^{coll} \approx 1$, and according to eq 7 marks the crossover from MF to DC kinetics. Using the above expression for $\mathcal{N}^{coll}$ and the melts result $P_{eq}^{cont} = h^3/V$, eq 7 then leads to an expression for k of exactly the type displayed in eq 8:

$$k_{un} \approx \begin{cases} \tilde{Q}h^3, & N \ll N_{un}^* \\ (t_h^{-1}h^3)N^{-1/2}, & N \gg N_{un}^* \end{cases}, \qquad N_{un}^* \equiv (\tilde{Q}t_h)^{-2} \tag{19}$$

Reacting chains shorter than N_{un}^* obey MF kinetics, while longer chains follow the DC result first obtained by Doi.[19] Note that the smaller the reactivity of the groups, the longer the chains must be before the DC regime is realized. An interesting aspect of the DC result is that all details of the chemical groups disappear.

Now entangled melts[20] ($N > N_e^{melts}$) are more complex since a number of distinct $t < \tau$ regimes exist, each with its own value of θ. We employ the framework of the reptation model[17,18] following de Gennes, who has discussed[20] the form of the time integral of $S(t)$ in this case, finding for large N a dominant contribution approximately equal to $\tau/(R/h)^3$ where τ is the longest relaxation time, or "reptation time":

$$\tau = \tau_{rep} \approx t_h N^3/N_e^{melts} \tag{20}$$

Observing that the ideal statics are unaffected by entanglements, and adding the small time ($t \lesssim t_h$) contribution to $\int_0^\infty S$, namely, Bt_h where B is the constant in eq 6, this leads to $\mathcal{N}^{coll} \approx N^{3/2}/N_e^{melts}$. Thus, as for the unentangled case, many collisions occur during one coil–coil collision time and kinetics are driven to DC form by increasing chain length:

$$k_{ent} \approx \begin{cases} \tilde{Q}h^3, & N \ll N_{ent}^* \\ (t_h^{-1}h^3N_e^{melts})N^{-3/2}, & N \gg N_{ent}^* \end{cases}, \qquad N_{ent}^* \equiv (N_e^{melts}/\tilde{Q}t_h)^{2/3} \tag{21}$$

The crossover scale is now N_{ent}^* and the asymptotic DC result of de Gennes[20] involves a stronger power, $k_{ent} \sim 1/N^{3/2}$.

B. Dilute Solutions ($\theta > 1$). Dilute solutions exhibit long chain kinetics[22] quite different from those in melts because $\mathcal{N}^{coll}$ becomes small for large N. There are two reasons for this: the relaxation time[17] is reduced by hydrodynamic interactions ($\tau \sim R^3$ which means $z = 3$) and excluded volume reduces the contact probability (g

$\neq 0$). It follows[22,27] that $\theta = 1 + g/3$, so $\mathcal{N}^{coll}$ is now a *decreasing* function of N:

$$\mathcal{N}^{coll} \approx (\tau/t_h)^{-g/3} \approx N^{-3g/5} \tag{22}$$

We have used $R = hN^{\nu}$ where $\nu \approx 3/5$ is the Flory exponent.[17] From eq 7 it is clear that for large enough N kinetics are driven to the MF form of eq 8:

$$k \approx \tilde{Q}h^3N^{-3g/5}, \qquad N \gg N^*_{dil} \equiv (\tilde{Q}t_h)^{5/3g} \tag{23}$$

where eq 2 was used. Note that now the properties of the functional groups are involved, $\tilde{Q}$ and h, in contrast to melts where all such details disappeared for long enough chains.

For very weakly reactive groups (large activation barrier, $Q \ll t_h^{-1}$ whence $\tilde{Q} \approx Q$) one has $k \approx Qh^3N^{-3g/5}$ which, in common with all MF forms, is independent of any dynamical properties such as solvent viscosity η. The influence of excluded volume on dilute solution kinetics when weakly reactive groups are involved is the "kinetic excluded volume effect" of Morawetz.[14,45] The N dependence in this case, $k \sim N^{-3g/5}$, was first calculated by Khokhlov.[21]

In the limit of very reactive groups ($Q \gtrsim t_h^{-1}$, $\tilde{Q} \approx t_h^{-1}$) the molecular weight dependence is unchanged but the prefactor now involves the local viscosity-dependent dynamical scale $t_h \approx \eta h^3/k_BT$ where k_BT is the thermal energy factor. Thus $k \approx (h^3/t_h)N^{-3g/5}$, or

$$k \approx (kT/\eta)\, N^{-3g/5} \qquad \text{(strongly reactive groups)} \tag{24}$$

leading to[22] $k \sim N^{-0.15}$, $N^{-0.26}$, and $N^{-0.48}$ for end groups, one end and one internal, and two internal groups, respectively. One should note, however, that for end groups $\mathcal{N}^{coll} \approx N^{-0.15}$ which implies a very slow approach to the asymptotic MF kinetics since $k = \tilde{Q}h^3N^{-0.15}/(1 + \tilde{Q}t_h\mathcal{N}^{coll})$. For a given value of N, the correction to the asymptotic result depends sensitively on the nonuniversal constant B involved in $\tilde{Q}$ (see eq 7).

V. Concentration Effects: Unentangled Solutions

What happens to reaction kinetics as ϕ increases from dilute solution into the semidilute regime? We postpone the treatment of entanglements until section VI, considering for now solutions of polymers shorter than the entanglement threshold. It is well-known[17,18] that at concentrations above the overlap threshold $\phi = \phi^* \approx N^{-4/5}$, hydrodynamic and excluded volume interactions are screened out on scales greater than the screening length $\xi \approx h\phi^{-3/4}$. This is reflected in the equilibrium pair distribution function,[25] which exhibits the correlation hole effect (see eq 11) only on scales smaller than the screening length:

$$P_{eq}(r) \approx \begin{cases} (r/\xi)^g/V, & r < \xi \\ 1/V, & r > \xi \end{cases} \tag{25}$$

and in the coil size and relaxation time[17]

$$R = (N/s)^{1/2}\xi, \qquad \tau = (N/s)^2\tau_\xi, \qquad \tau_\xi \approx t_h(\xi/h)^3 \tag{26}$$

where s is the number of monomers per "blob" of size ξ. Each blob is swollen due to excluded volume interactions, $\xi \approx hs^{3/5}$, whence $s \approx \phi^{-5/4}$. The expression for τ is the Rouse result for N/s blobs each having relaxation time τ_ξ, and τ_ξ is the standard dilute hydrodynamics-dominated expression.

There are two candidates for k: the MF result and the DC result (see eq 8). From the expressions above, these read

$$k^{MF} = \tilde{Q}VP_{eq}^{cont} = \tilde{Q}h^3(h/\xi)^g, \qquad k^{DC} = \frac{R^3}{\tau} = \frac{h^3}{t_h}\left(\frac{s}{N}\right)^{1/2} \tag{27}$$

where the contact probability is obtained by integrating $P_{eq}(r)$ over scales $r < h$. Which of these two forms is the realized one? As always, to answer this one needs the mean number of functional group collisions when two reactive polymers meet. Using eq 6, one finds this is given by

$$\mathcal{N}^{coll} \approx N^{1/2}\,\phi^{(5+6g)/8} \approx N^{1/2}\phi^{0.8} \qquad \text{(end groups)} \tag{28}$$

The important property is that $\mathcal{N}^{coll}$ is an increasing function of both molecular weight and concentration. This implies that, at fixed chain length, increasing ϕ will eventually *drive* kinetics to DC form. That is, the dilute MF kinetics which we have established in the previous section, and which must prevail at the lowest concentrations in the semidilute regime, must cross over to DC form at a certain concentration $\phi = \phi^{**}_{un}$. This is the concentration at which the total reaction probability first reaches unity:

$$\tilde{Q}t_h\mathcal{N}^{coll} \approx (\phi/\phi^{**}_{un})^{(5+6g)/8},$$
$$\phi^{**}_{un} \equiv \{(\tilde{Q}t_h)^2N\}^{-4/(5+6g)} \sim N^{-0.6} \qquad \text{(end groups)} \tag{29}$$

Thus, for chains of a given length N, we expect MF kinetics when $\phi < \phi^{**}_{un}$ and DC kinetics when $\phi > \phi^{**}_{un}$:

$$k \approx \begin{cases} (\tilde{Q}h^3)\phi^{3g/4}, & \phi \ll \phi^{**}_{un} \\ (t_h^{-1}h^3)\phi^{-5/8}N^{-1/2}, & \phi \gg \phi^{**}_{un} \end{cases} \tag{30}$$

where we have rewritten the forms exhibited in eq 27 in terms of concentration ϕ. This implies that near the beginning of the semidilute regime the rate constant increases as $k \sim \phi^{0.19}$ (taking end groups as an example). At concentrations above ϕ^{**}_{un}, k then decreases under DC kinetics. Thus k is peaked at $\phi \approx \phi^{**}_{un}$ which, in accord with experiment,[10,11] is distinct from the overlap threshold ϕ^*.

The arguments of this section are made more rigorous in Appendix B, where $S(t)$ is derived and its time integral is shown to lead to precisely the result for $\mathcal{N}^{coll}$ displayed in eq 28. Inserting this into the general result of eq 7 yields the complete expression for k which interpolates between the MF and DC limits in eq 30:

$$k = \frac{k^{dil}(\phi/\phi^*)^{3g/4}}{1 + (\phi/\phi^{**}_{un})^{(3g/4+5/8)}}, \quad k^{dil} \equiv \tilde{Q}h^3N^{-3g/5} \quad (\phi > \phi^*) \tag{31}$$

where k^{dil} is the large-N dilute solution result which applies for $\phi < \phi^*$.

VI. Concentration Effects: Entangled Solutions

This section addresses the reaction kinetics of chains which are strongly entangled, i.e., which are longer than a certain threshold[44] $N_e(\phi)$. We will assume power law behavior:

$$N_e(\phi) = N_e^{melts}\phi^{-\gamma} \tag{32}$$

such that the number of entanglements restricting a polymer of fixed length N grows as ϕ^γ where experimental values[44,46-49] lie in the range $1 \lesssim \gamma \lesssim 1.3$.

Our framework is the reptation model.[18,17] In the "melt of blobs" picture one simply carries over melt reptation dynamics to entangled solutions by replacing $N \to N/s$, $N_e \to N_e/s$, $h \to \xi$, and $t_h \to \tau_\xi$ since each chain possesses N/s blobs of size ξ and relaxation time τ_ξ. These are viewed as the new "monomers" in an entangled "melt". Thus the melts reptation time of eq 20 is replaced by

$$\tau_{rep} = \tau_\xi N^3/(N_e(\phi)s^2) \tag{33}$$

with sub-blob scales obeying dilute solution statics and dynamics. In appendix C the time integral of $S(t)$ is derived, leading to a result for $\mathcal{N}^{coll}$ which as expected is of the form shown in eq 6. Noting that R and P_{eq}^{cont} are unchanged from the unentangled case, and making use of eq 33, one finds

$$\mathcal{N}^{coll} \approx \frac{N^{3/2}}{N_e^{melts}}\phi^{\gamma+(5+6g)/8} \sim N^{3/2}\,\phi^{1.8} \qquad \text{(end groups)} \tag{34}$$

where we have estimated the power of ϕ by taking a typical value $\gamma = 1$. Again, the essential feature is that $\mathcal{N}^{coll}$ is an *increasing* function of ϕ; at low concentrations the same MF law applies as for unentangled solutions, but increasing concentration eventually drives kinetics to DC behavior, $k = k^{DC} = R^3/\tau_{rep}$:

$$k \approx \begin{cases} (\tilde{Q}h^3)\phi^{3g/4}, & \phi \ll \phi_{ent}^{**} \\ (t_h^{-1}h^3 N_e^{melts})\phi^{-(5/8+\gamma)}N^{-3/2}, & \phi \gg \phi_{ent}^{**} \end{cases} \tag{35}$$

The crossover, again determined by equating $\tilde{Q}t_h\mathcal{N}^{coll}$ to unity, is now at $\phi = \phi_{ent}^{**}$ where

$$\phi_{ent}^{**} \equiv \{(\tilde{Q}t_h/N_e^{melts})^{2/3}N\}^{-12/(5+6g+8\gamma)} \tag{36}$$

The full trajectory of k as ϕ increases from the overlap threshold is given by eq 7 and interpolates between these limiting behaviors:

$$k \approx \frac{k^{dil}(\phi/\phi^*)^{3g/4}}{1 + (\phi/\phi_{ent}^{**})^{3g/4+5/8+\gamma}} \quad (\phi > \phi^*) \tag{37}$$

The high-concentration DC kinetics now involve sharper decays, $k \sim \phi^{-1.6}N^{-3/2}$ for $\gamma = 1$. This is the influence of entanglements which retard reaction rates. The rate constant is peaked at a concentration $\phi \approx \phi_{ent}^{**} \sim N^{-0.8}$ for end groups.

VII. Weak and Strong Systems

The main objective of this paper is to determine how k varies as a function of concentration ϕ at fixed chain length N. This is what is measured in the phosphorescence experiments of Figure 2a. So far, we have established that below the overlap threshold ϕ^* the rate constant is essentially a constant, k^{dil}. Above ϕ^*, it starts to increase because MF kinetics are obeyed; a transition to DC behavior then occurs at either $\phi = \phi_{un}^{**}$ or ϕ_{ent}^{**} depending on whether the chains are entangled or not at the transition.

For a given experimental system, does the transition occur at ϕ_{un}^{**} or at ϕ_{ent}^{**}? We will see below that this depends on whether the system is a "weak" one or a "strong" one. The realized "trajectory" of $k(\phi)$ for a fixed N depends on the concentration ϕ_e at which entanglements onset, determined by $N_e(\phi_e) \equiv N$. Thus

$$\phi_e = (N_e^{melts}/N)^{1/\gamma} \tag{38}$$

With typical values $\gamma \approx 1$, one has roughly $\phi_e \propto 1/N$. Now the observed behavior of k is governed by the relationship between ϕ_e and the MF $\to$ DC crossover values ϕ_{un}^{**} and ϕ_{ent}^{**}. In fact, from the expressions in eqs 29, 36, and 38 an important relationship follows:

$$\phi_{un}^{**}\phi_e = (\phi_{ent}^{**})^{1+w}, \qquad w \equiv 8\gamma/(5+6g) \tag{39}$$

This result implies that ϕ_{ent}^{**} *always lies between* ϕ_{un}^{**} *and* ϕ_e. *Thus there are only two possibilities, which we label respectively "strongly reactive" and "weakly reactive" as follows.*

A. Strong Systems: $\phi_{un}^{**} < \phi_{ent}^{**} < \phi_e$. Here reactions are sufficiently "strong" that the MF $\to$ DC transition occurs, as ϕ is increased at fixed N, *before* the onset of entanglements: $\phi_{un}^{**} < \phi_e$. The observed behavior, therefore, will initially be that for unentangled solutions, eq 31, with k exhibiting a peak around $\phi = \phi_{un}^{**}$. As soon as entanglements become important, at $\phi = \phi_e$, we then cross *directly* into the entangled DC regime of eq 35 since $\phi_{ent}^{**} < \phi_e$. The predicted behavior is therefore

$$k \approx \begin{cases} (\tilde{Q}h^3)N^{-3g/5}, & \phi \ll \phi^* \\ (\tilde{Q}h^3)\phi^{3/4}, & \phi^* \ll \phi \ll \phi_{un}^{**} \\ (t_h^{-1}h^3)\phi^{-5/8}N^{-1/2}, & \phi_{un}^{**} \ll \phi \ll \phi_e \\ (t_h^{-1}h^3 N_e^{melts})\phi^{-(5/8+\gamma)}N^{-3/2}, & \phi_e \ll \phi \end{cases}$$

(strong) (40)

Of course, for chains which are so short that $N < N_e^{melts}$, entanglements never feature and the observed behavior then corresponds only to the $\phi < \phi_e$ regimes in eq 40.

B. Weak Systems: $\phi_e < \phi_{ent}^{**} < \phi_{un}^{**}$. In these cases reactions are sufficiently weak that entanglements onset before DC kinetics apply. Thus the entire trajectory of k is that described by the entanglements picture, eq 35:

$$K \approx \begin{cases} (\tilde{Q}h^3)N^{-3g/5}, & \phi \ll \phi^* \\ (\tilde{Q}h^3)\phi^{3g/4}, & \phi^* \ll \phi \ll \phi_{ent}^{**} \\ (t_h^{-1}h^3 N_e^{melts})\phi^{-(5/8+\gamma)}N^{-3/2}, & \phi_{ent}^{**} \ll \phi \end{cases}$$

(weak) (41)

VIII. Comparison with Experiment and Discussion

The main experimental predictions of this work are eqs 40 and 41, describing the concentration dependence of the rate constant for strong and weak systems, respectively. A priori, one does not know to which class an experimental system belongs, this depending on the magnitudes of the group reactivity measured by $\tilde{Q}t_h$ and on N_e^{melts} and N. The class must be inferred from experimental data. Note that the dependence on reactive group location along the chain backbone arises through the correlation hole exponent g. With free radical polymerization in mind, let us specialize our results to end groups, for which $g \approx 1/4$. In this case, for a weak system we predict (see eqs 41 and 36)

$$k(t_h/h^3) \approx \begin{cases} (\tilde{Q}t_h)N^{-0.15}, & \phi \ll \phi^* \\ (\tilde{Q}t_h)\phi^{0.19}, & \phi^* \ll \phi \ll \phi_{ent}^{**} \sim N^{-0.83} \\ N_e^{melts}\phi^{-1.6}N^{-3/2}, & \phi_{ent}^{**} \ll \phi \end{cases}$$

(weak, end groups) (42)

where we have taken $\gamma \approx 1$ for the entanglement exponent. The above k vs ϕ behavior is shown in Figure 2b; where the full theoretical trajectories according to eq 37 have been plotted for a range of N values, each curve beginning at $\phi = \phi^*$. For the chosen group reactivity $\tilde{Q}t_h = 0.1$ and entanglement parameters ($N_e^{melts} = 200$, a "typical" value,[44] and $\gamma = 1$) these are all weak systems, obeying eq 42. The important features are the slopes of 0.19 and −1.6 for small and large concentrations, respectively, and the fact that the MF → DC transition occurs at a concentration which is a decreasing function of N and does *not* coincide with the overlap threshold ϕ^*.

Let us compare these curves with the experimental phosphorescence quenching results of Mita et al. shown in Figure 2a which correspond to their two longest polystyrene in benzene samples.[10] The data are rather difficult to compare quantitatively to theory since the reacting chains are of different lengths to one another, with inert background chains of yet a third length (generally one expects[22] the smallest of the reacting chains to dominate k). For the longest chain sample in Figure 2a the peak in k clearly occurs at a concentration considerably greater than the overlap threshold ϕ^*. The large ϕ reaction rates exhibit a slope slightly less than −1.6 which in our picture suggests $\gamma \approx 1$; this in turn leads to $\phi_e \approx 0.05$ for the higher molecular weight specimens, if one takes[44] $N_e^{melts} \approx 200$, suggesting a weak system (ϕ_e being less than the ϕ value at which k is peaked). With[50] $h \approx 5.5$ Å and $t_h \approx 2 \times 10^{-11}$ s estimated[10] from benzene viscosity data, one has $h^3/t_h \approx 5 \times 10^9$ L mol^{-1} s^{-1} which is close to the value reported[9] in dilute solution for $N = 1$. Comparing to the dilute solution values for k in Figure 2a (those data points to the left of the peaks) suggests, very roughly indeed, $\tilde{Q}t_h \approx 0.5$. While there are no measurements in the region between these points and the peak values, the experimental increase in k across that region is certainly greater than our theory would suggest according to the MF kinetics expected to apply there. In fact, the dilute solution phosphorescence data reported elsewhere[9] for the same system follow a stronger power than $k \sim N^{-0.15}$, so discrepancy in that region is perhaps not surprising. This may result from the chains being insufficiently long to probe the asymptotic regime in which excluded volume statistics pertain; indeed, radical combination rates in dilute polyoxyethylene solution[51] suggest a significantly smaller power which is close to the theoretical value.

Our predictions for reactive groups positioned away from chain ends involve very different power laws at lower concentrations. For example, consider the case of very reactive groups ($\tilde{Q}t_h \to 1$) both deeply internal along the backbone. Now $g \approx 0.8$ is much bigger and from eqs 29 and 40 with $\gamma \approx 1$, one has for the case of a strong system

$$k(t_h/h^3) \approx \begin{cases} (\tilde{Q}t_h)N^{-0.48}, & \phi \ll \phi^* \\ (\tilde{Q}t_h)\phi^{0.6}, & \phi^* \ll \phi \ll \phi_{un}^{**} \sim N^{-0.41} \\ \phi^{-0.63}N^{-1/2}, & \phi_{un}^{**} \ll \phi \ll \phi_e = N^{-1}N_e^{melts} \\ N_e^{melts}\phi^{-1.6}N^{-3/2}, & \phi_e \ll \phi \end{cases} \quad \text{(strong, internal groups)} \quad (43)$$

We conclude with a summary of the ideas developed in this study. The essential quantity is the mean number of functional group collisions $\mathcal{N}^{coll}$, whose dependence on chain length is very different in dilute solutions and entangled melts:

$$\mathcal{N}^{coll} = \begin{cases} (N_e^{melts})^{-1}N^{3/2}, & \text{entangled melts} \\ N^{-3g/5}, & \text{dilute solutions} \end{cases} \quad (44)$$

Therefore in melts increasing chain length drives reaction kinetics to the DC limit, because reaction is almost certain to occur if ever two reactive polymers meet. Dilute solutions are driven in the "opposite direction" to MF kinetics; reaction is unlikely for long chains.

At finite concentrations, kinetics are closely related to those in melts and dilute solutions. These latter determine respectively the *large* and the *small* scale features of the kinetics, as is clearly manifested in the structure of $\mathcal{N}^{coll}$:

$$\mathcal{N}^{coll} = \frac{s}{N_e}\left(\frac{N}{s}\right)^{3/2} s^{-3g/5} \sim N^{3/2}\phi^w \quad (45)$$

where $w \equiv \gamma + (5+6g)/8$. A reactive polymer may be thought of as comprising N/s blobs, each containing s monomers, where the blob size is equal to the screening length ξ. Statics and dynamics[17] are known to be melt-like (dilute-like) on scales larger (smaller) than the blob size. Correspondingly, the above expression for $\mathcal{N}^{coll}$ is simply the melts result, with N and N_e replaced by N/s and N_e/s, multiplied by the dilute solution result, with N replaced by s. That is, the number of collisions equals the number of times the "reactive blobs" collide (i.e., the blobs containing the active chain units) multiplied by the number of times the reactive groups collide each time their host blobs collide.

Since the number of chain units per blob is reduced ($s \approx \phi^{-5/4}$), eq 45 tells us that the effect of increasing concentration is to *increase* $\mathcal{N}^{coll}$. This increase results from two physical consequences of higher concentration: (1) the reactive group contact probability when two live coils are overlapped is greater due to screening of excluded volume repulsions; (2) the coil relaxation time is increased because hydrodynamical interactions are screened and because the number of entanglements per chain is higher. The second effect means there is more time for the reactive groups to meet one another since the overlap and relaxation times are essentially equal. Thus, the MF kinetics which are obeyed at concentrations close to the dilute limit are eventually driven to DC behavior at a certain threshold concentration. This MF → DC transition is the origin of the peak observed in the rate constant, shown in Figure 2.

In Figure 3 a simple picture of reacting polymers in semidilute solution is shown, which captures the large scale melt-like behavior. The situation is analogous to a melt of blobs in which each live chain has one reactive blob with effective reactivity Q_{eff} instead of $\tilde{Q}$. Q_{eff} is determined by the *small-scale* dilute solution kinetics, $Q_{eff} = \tilde{Q}(h/\xi)^{3+g}$, and is reduced from $\tilde{Q}$ by a factor equal to the reactive group contact probability *given* that the two reactive blobs overlap one another. That this reduction factor is a conditional equilibrium contact probability (as opposed to a ratio of time scales) is a direct consequence of the fact that dilute solution kinetics, which apply on scales smaller than ξ, are of MF type. One can then show that all of the semidilute results for k of sections V and VI can be obtained from the results for *melts* of section IV by replacing $N \to N/s$, $h \to \xi$, $t_h \to \tau_\xi$ and $\tilde{Q} \to Q_{eff}$.

It is hoped that the results presented here will help to motivate further experiment. Systematic studies of reaction rates in monodisperse systems are needed, ideally in parallel with coil size and relaxation time measurements on the same polymer–solvent systems but without reactive

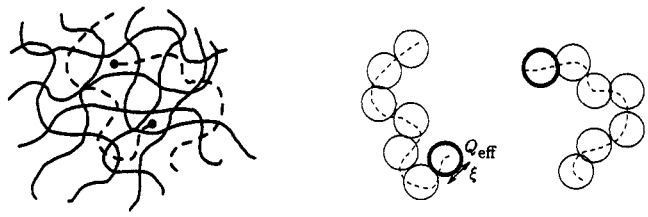

(a) (b)

Figure 3. (a) Pair of reacting polymers (with reactive end groups) in a semidilute environment whose correlation length or "mesh spacing" is ξ. This situation is analogous to a reacting pair in the *melt*, depicted in (b), where the "monomers" are blobs of size ξ and the "reactive blobs" are of effective reaction range ξ and reactivity Q_{eff}.

groups. From the point of view of applications, end groups are probably of most significance given their role in free radical polymerization. However, studies of reactions between strongly reactive internally positioned species have the advantage that the power laws both in dilute solution and at lower semidilute concentrations are much stronger (see eq 43). Not only are stronger powers more easily measured, but they also imply faster crossover to the asymptotic long chain regimes. Studies such as these would provide strong tests of the theory developed in this paper.

Acknowledgment. This work was supported by the National Science Foundation under Grant No. CTS-89-08995. Helpful discussions with Jane Yu are gratefully acknowledged.

Appendix A. Derivation of General Result for k

In this appendix we will obtain the result of eq 4 from eq 3. Now for $(t-t') \gg t_h$, where t_h is the microscopic relaxation time of one chain unit, we can replace $G(r,r',t-t') \rightarrow G(r,0,t-t')$ in eq 3 with negligible error since for such times G is almost flat in the domain $|r'| < h$. On the other hand for $(t-t') \ll t_h$ since G is then normalized with respect to r over a region much smaller than h, we have $\int_{|r|<h} d^3r\, G(r,r',t-t') \approx 1$ for most $|r'| < h$. Then it follows from integrating eq 3 over r values within h of the origin that

$$P_t^{cont} \approx P_{eq}^{cont} - Qh^3 \int_0^t dt'\, S(t-t') P_{t'}^{cont} \qquad \text{(A1)}$$

where the return probability $S(t)$ is defined in eq 5 and $P_t^{cont} \equiv \int_{|r|<h} d^3r\, P_t(r)$ is the probability that the reactive groups of a pair of live chains are in contact at time t (with a similar definition for P_{eq}^{cont}).

Taking the time derivative of the normalization of eq 3, one finds $\dot{\Gamma}_t = QP_t^{cont}$, implying $k = QVP_t^{cont}$. Then Laplace transforming eq A1, $t \rightarrow E$, P_E^{cont} is easily solved for, leading to $k_E = QVP_{eq}^{cont}/[E(1 + QS(E))]$. Taking the limit $E \rightarrow 0$, one obtains the expression for the long time rate constant of eq 4.

Appendix B. Time Integral of $S(t)$: Unentangled Solutions

Corresponding to the small scale dilute-like and large-scale melt-like regimes of statics and dynamics, unentangled semidilute reaction kinetics are characterized by two distinct values of θ: $\theta_1 = 1 + g/3$ and $\theta_2 = 3/4$ (see section IV). The requirement of continuity in $S(t)$ then dictates the following form:

$$S(t) \approx \begin{cases} 1, & t < t_h \\ (t/t_h)^{-\theta_1}, & t_h < t < \tau_\xi \\ (\xi/R)^3 (h/\xi)^{3+g} (t/\tau)^{-\theta_2}, & \tau_\xi < t < \tau \\ (\xi/R)^3 (h/\xi)^{3+g} (t/\tau)^{-3/2}, & \tau < t \end{cases} \qquad \text{(B1)}$$

These expressions are easily understood by noting that the prefactor for $t > \tau_\xi$ is the *conditional* contact probability, between two reactive groups, *given* that the groups are within R of one another (i.e., that the host coils overlap one another):

$$P_{eq}(r<h|r<R) = P_{eq}(r<h)/P_{eq}(r<R) \approx \left(\frac{\xi}{R}\right)^3 \left(\frac{h}{\xi}\right)^{3+g} \qquad \text{(B2)}$$

where we have used eq 25 and $h \ll \xi \ll R$ is always assumed. Here $P_{eq}(r<x) \equiv \int_{|r|<x} P_{eq}(r)$ denotes the sum over all separations less than x. Equation B1 can then be obtained by requiring that $S(\tau) \approx P_{eq}(r<h|r<R)$. Integrating, one finds

$$\int_0^\infty S(t)\, d(t/t_h) \approx B + \tau/t_h \left(\frac{\xi}{R}\right)^3 \left(\frac{h}{\xi}\right)^{3+g} [1 + \mathcal{O}(\phi/\phi^*)^{-5/8}] \qquad \text{(B3)}$$

where B is a constant of order unity. From eq 6 this identifies $\mathcal{N}^{coll} \approx (\tau/t_h)(\xi/R)^3 (h/\xi)^{(3+g)}$ at concentrations well above the overlap threshold. This leads to eq 28.

Appendix C. Time Integral of $S(t)$: Entangled Solutions

The procedure is very close to that used by de Gennes in his study of melts[20] except that one replaces monomers with "blobs" of size ξ. Now in the reptation model[17,18] the lateral chain motion is hindered by a tube of size $b \approx (N_e/s)^{1/2}\xi$ on time scales greater than $t_b \approx (N_e/s)^2 \tau_\xi$, while for $\tau_\xi < t < t_b$ unconstrained Rouse dynamics apply (rms monomer displacement $x_t \sim t^{1/4}$), i.e., $\theta_2 = 3/4$ since $g = 0$ for all scales greater than ξ (ideal statics). Beyond t_b the dynamics are those of a one-dimensional Rouse chain whose longest relaxation time is $T_R \approx (N/s)^2 \tau_\xi$, leading to $\theta_3 = 3/8$ for $t_b < t < T_R$ ($x_t \sim t^{1/8}$) and $\theta_4 = 3/4$ for $T_R < t < \tau_{rep}$ ($x_t \sim t^{1/4}$) where τ_{rep} is the reptation time of eq 33. At the shortest times $t < \tau_\xi$ we have $\theta_1 = 1 + g/3$ as in dilute solutions and center of gravity diffusion takes over at the longest, $\theta_3 = 3/2$. Thus the earliest two regimes up to τ_ξ are as in dilute solution ($S(t<t_h) \approx 1$, $S(t_h<t<\tau_\xi)$

$\approx (t/t_h)^{-\theta_1}$), and the remaining regimes read

$$S(t) \approx \begin{cases} P_{eq}(r<h|r<b)(t/t_b)^{-\theta_2}, & \tau_\xi < t < t_b \\ P_{eq}(r<h|r<b)(t/t_b)^{-\theta_3}, & t_b < t < T_R \\ P_{eq}(r<h|r<R)(t/\tau_{rep})^{-\theta_4}, & T_R < t < \tau_{rep} \\ P_{eq}(r<h|r<R)(t/\tau_{rep})^{-3/2} & \tau_{rep} < t \end{cases} \quad (C1)$$

where we have exploited the crossover requirements $S(t_b) \approx P_{eq}(r<h|r<b)$ and $S(\tau_{rep}) \approx P_{eq}(r<h|r<R)$. The latter conditional probability is given in eq B2 and a similar logic leads to $P_{eq}(r<h|r<b) \approx (\xi/b)^3(h/\xi)^{3+g}$. On integrating, for large N/N_e one finds that the $t > \tau_\xi$ regimes are dominant:

$$\int_0^\infty S(t) \approx Bt_h + \left(\frac{\xi}{R}\right)^3\left(\frac{h}{\xi}\right)^{3+g}\tau_{rep}\left[1 + \mathcal{O}\left(\frac{N_e}{N}\right)^{1/4}\right] \quad (C2)$$

where B is a constant of order unity. This identifies $\mathcal{N}^{coll}$ through eq 6, and for $N/N_e \gg 1$ one obtains eq 34.

References and Notes

(1) Flory, P. *Principles of Polymer Chemistry*; Cornell University Press: Ithaca, NY, 1971.
(2) Cardenas, J.; O'Driscoll, K. F. *J. Polym. Sci., Polym. Chem. Ed.* **1976**, *14*, 883.
(3) Marten, F. L.; Hamielec, A. E. *A.C.S. Symp. Ser.* **1979**, *104*, 43.
(4) O'Driscoll, K. F. *Pure Appl. Chem.* **1981**, *53*, 617.
(5) Tulig, T. J.; Tirrell, M. *Macromolecules* **1982**, *115*, 459.
(6) Mahabadi, H.-K. *Macromolecules* **1985**, *18*, 1319.
(7) Mahabadi, H.-K. *Macromolecules* **1991**, *24*, 606.
(8) Cuniberti, C.; Perico, A. *Eur. Polym. J.* **1977**, *13*, 369.
(9) Horie, K.; Mita, I. *Macromolecules* **1978**, *11*, 1175.
(10) Mita, I.; Horie, K.; Takeda, M. *Macromolecules* **1981**, *14*, 1428.
(11) Mita, I.; Horie, K. *J. Macromol. Sci., Rev. Macromol. Chem. Phys.* **1987**, *C27(1)*, 91.
(12) Gebert, M. S.; Yu, D. H. S.; Torkelson, J. M. *Macromolecules* **1992**, *25*, 4160.
(13) Gebert, M. S.; Torkelson, J. M. *Polymer* **1990**, *31*, 2402.
(14) Cho, J.; Morawetz, H. *Macromolecules* **1973**, *6*, 628.
(15) Cates, M. E.; Candau, S. F. *J. Phys.: Condens. Matter* **1990**, *2*, 6869.
(16) Clint, J. H. *Surfactant Aggregation*; Chapman and Hall: New York, 1992.
(17) de Gennes, P. G. *Scaling Concepts in Polymer Physics*; Cornell University Press: Ithaca, NY, 1985.
(18) Doi, M.; Edwards, S. F. *The Theory of Polymer Dynamics*; Clarendon Press: Oxford, 1986.
(19) Doi, M. *Chem. Phys.* **1975**, *11*, 115.
(20) de Gennes, P. G. *J. Chem. Phys.* **1982**, *76*, 3316, 3322.
(21) Khokhlov, A. R. *Makromol. Chem., Rapid Commun.* **1981**, *2*, 633.
(22) Friedman, B.; O'Shaughnessy, B. *Macromolecules* **1993**, *26*, 5726.
(23) de Gennes, P. G. *Radiat. Phys. Chem.* **1983**, *22*, 193.
(24) von Smoluchowski, M. *Z. Phys. Chem.* **1917**, *92*, 192.
(25) Witten, T. A.; Prentis, J. J. *J. Chem. Phys.* **1982**, *77*, 4247.
(26) des Cloizeaux, J. *J. Phys. (Paris)* **1980**, *41*, 223.
(27) Friedman, B.; O'Shaughnessy, B. *Macromolecules* **1993**, *26*, 4888.
(28) Friedman, B.; O'Shaughnessy, B. *Europhys. Lett.* **1993**, *23*, 667.
(29) Schafer, L.; Vonferber, C.; Lehr, U.; Duplantier, B. *Nucl. Phys. B* **1992**, *374*, 473.
(30) Duplantier, B. *J. Stat. Phys.* **1989**, *54*, 581.
(31) North, A. M.; Reed, G. A. *Trans. Faraday Soc.* **1961**, *57*, 859.
(32) Kent, M. S.; Faldi, A.; Tirrell, M.; Lodge, T. P. *Macromolecules* **1992**, *25*, 4501.
(33) Kent, M. S.; Tirrell, M.; Lodge, T. P. *Macromolecules* **1992**, *25*, 6240.
(34) Tulig, T. J.; Tirrell, M. *Macromolecules* **1981**, *14*, 1501.
(35) Gebert, M. S.; Torkelson, J. M. *Polymer* **1990**, *31*, 2402.
(36) O'Shaughnessy, B. *Phys. Rev. Lett.* **1993**, *71*, 3331.
(37) Wilemski, G.; Fixman, M. *J. Chem. Phys.* **1974**, *60*, 866, 878.
(38) Doi, M. *Chem. Phys.* **1975**, *9*, 455.
(39) Perico, A.; Cuniberti, C. *J. Polym. Sci., Polym. Phys. Ed.* **1977**, *15*, 1435.
(40) O'Shaughnessy, B. *J. Chem. Phys.* **1991**, *94*, 4042.
(41) Friedman, B.; O'Shaughnessy, B. *Phys. Rev. Lett.* **1988**, *60*, 64.
(42) Friedman, B.; O'Shaughnessy, B. *J. Phys. II (Paris)* **1991**, *1*, 471.
(43) Friedman, B.; O'Shaughnessy, B. *Europhys. Lett.* **1993**, *21*, 779.
(44) Ferry, J. D. *Viscoelastic Properties of Polymers*, 3rd ed.; John Wiley and Sons: New York, 1980.
(45) Wang, Y.; Morawetz, H. *Macromolecules* **1990**, *23*, 1753.
(46) Graessley, W. W.; Edwards, S. F. *Polymer* **1981**, *22*, 1329.
(47) Klein, J. *Macromolecules* **1978**, *11*, 852.
(48) Richards, W. D.; Prud'homme, R. K. *J. Appl. Polym. Sci.* **1986**, *31*, 763.
(49) Tirrell, M. *Rubber Chem. Technol.* **1986**, *57*, 523.
(50) Brandrup, J.; Immergut, E. H. *Polymer Handbook*, 3rd ed.; Wiley: New York, 1966.
(51) Borgwardt, U.; Schnabel, W.; Henglein, A. *Makromol. Chem.* **1969**, *127*, 176.